Oil-palm management alters the spatial distribution of amorphous silica and mobile silicon in topsoils

Britta Greenshields[1], Barbara von der Lühe[1*], Harold J. Hughes[1], Christian Stiegler[2], Suria Tarigan[3], Aiyen Tjoa[4], Daniela Sauer[1]

[1]Department of Physical Geography, University of Göttingen, Göttingen, 37077, Germany
*Now at the Faculty of Geoscience, University of Münster, Münster, 48149, Germany
[2]Bioclimatology, Büsgen Institute, University of Göttingen, Göttingen, 37077, Germany
[3]Department of Soil and Natural Resources Management, IPB University, Dramaga Bogor, 16680, Indonesia
[4]Department of Agrotechnology, Tadulako University, Palu, 94118, Indonesia

Correspondence to: Britta Greenshields (britta.greenshields@uni-goettingen.de)

Abstract. Effects of oil-palm (*Elaeis guineensis* Jacq.) management on silicon (Si) cycling under smallholder oil-palm plantations have hardly been investigated. As oil palms are Si accumulators, we hypothesized that management practices and topsoil erosion may cause Si losses and changes in spatial Si concentration patterns in topsoils under oil-palm cultivation. To test this hypothesis, we took topsoil samples under mature oil-palm plantations in well-drained and riparian areas of Jambi Province, Indonesia. The samples were taken from four different management zones within each oil-palm plot: palm circles, oil-palm rows, interrows and below frond piles. We quantified mobile Si (Si_M) and Si in amorphous silica (Si_{Am}) by $CaCl_2$ and $NaCO_3$ extraction, respectively. Both fractions are important Si pools in soils and are essential for plant-soil Si cycling. We further installed sediment traps on sloping, well-drained oil-palm plantations to estimate the annual loss of soil and Si_{Am} caused by erosion. In well-drained areas, mean topsoil Si_{Am} concentrations were significantly higher below frond piles (3.97 ± 1.54 mg g^{-1}) compared to palm circles (1.71 ± 0.35 mg g^{-1}), oil-palm rows (1.87 ± 0.51 mg g^{-1}) and interrows (1.88 ± 0.39 mg g^{-1}). In riparian areas, highest mean topsoil Si_{Am} concentrations were also found below frond piles (2.96 ± 0.36 mg g^{-1}) and in grass-covered interrows (2.71 ± 0.13 mg g^{-1}), whereas topsoil Si_{Am} concentrations of palm circles were much lower (1.44 ± 0.55 mg g^{-1}). We attributed the high Si_{Am} concentrations in topsoils under frond piles and in grass-covered interrows to phytolith release from decaying oil-palm fronds, grasses, and sedges. The significantly lower Si_{Am} concentrations in palm circles (in both well-drained and riparian areas), oil-palm rows and unvegetated interrows (only in well-drained areas) were explained by a lack of litter return to these management zones. Mean topsoil Si_M concentrations were in a range of ~10 – 20 µg g^{-1}. They tended to be higher in riparian areas, but the differences between well-drained and riparian sites were not statistically significant. Soil-loss calculations based on erosion traps confirmed that topsoil erosion was considerable in oil-palm interrows on slopes. Erosion estimates were in a range of 4 – 6 Mg ha^{-1} yr^{-1}, involving Si_{Am} losses in a range of 5 – 9 kg^{-1} ha^{-1} yr^{-1}. Based on the observed spatial Si patterns, we concluded that smallholders could efficiently reduce erosion and support Si cycling within the system by (1) maintaining a vegetation cover in oil-palm rows and interrows, (2) incorporating oil-palm litter into farm management and (3) preventing soil compaction and surface-crust formation.

Keywords: oil-palm plantations, oil-palm management, silicon pools, phytoliths, topsoil erosion, silicon extraction

1 Introduction

40 Lowland-rainforest transformation to cash-crop plantation systems (e.g., timber, rubber, and oil palm) involves vast expansion of oil-palm monocultures in Jambi Province, Indonesia (Drescher et al., 2016; Tsujino et al., 2016). By now, smallholder farmers manage 40 % of oil-palm plantations in Jambi Province (Euler et al., 2016), whereby palm oil remains a tropical cash crop with high demand on the global market (FAO 2020). Oil-palm cultivation has improved the livelihoods of many smallholder farmers, yet at the expense of the natural environment (Clough
45 et al., 2016; Grass et al., 2020; Qaim et al., 2020), leading to a decrease in biodiversity (Drescher et al., 2016; Meijaard et al., 2020) and ecosystem services (Dislich et al., 2017). Due to these "trade-offs" (Grass et al., 2020) and a global interest to reduce deforestation (Tsujino et al., 2016), much research focuses on identifying ways to increase land-use sustainability while keeping current oil-palm plantations profitable (Darras et al., 2019; Luke et
50 al., 2019).

Under humid-tropical climate conditions, intense silicate weathering and element leaching from soils takes place, including leaching of silicon (Si), i.e., desilification (Haynes, 2014). Farmers commonly apply nitrogen-phosphorous-potassium (NPK) fertilizers and lime to maintain an adequate plant nutrition and soil pH (Darras et al., 2019). However, Si also plays an important role in terrestrial biogeochemical cycling (Struyf and Conley,
55 2012) and enhances crop production in several ways (Epstein, 2009; Guntzer et al., 2012). In soils, silicic acid can mobilize phosphate by occupying anion adsorption sites. Si also mitigates plant toxicity by binding toxic cations such as aluminium (Al), cadmium (Cd), and arsenic (As) that become mobile at low soil pH (Schaller et al., 2020; Street-Perrott and Barker, 2008). Furthermore, Si can increase drought resistance of plants (Schaller et al., 2020). Silica precipitates in cell walls, cell lumen and intercellular spaces of leaves and can reduce transpiration (Epstein,
60 2009). In Si-depleted soils, some crops, including oil palms, can thus benefit from Si fertilization (Klotzbücher et al., 2018).

In terrestrial ecosystems, Si cycling is mostly driven by two Si pools: mobile Si in soil solution (Si_M) and Si present in amorphous silica (Si_{Am}) (Struyf et al., 2010; de Tombeur et al., 2020). Si_M is the Si fraction that is readily available to plants and usually present as monomeric silicic acid (H_4SiO_4) in terrestrial environments (Georgiadis
65 et al., 2013). Si_{Am} is the largest non-mineral Si pool in soils (Barão et al., 2014; Unzué-Belmonte et al., 2017). Its solubility exceeds that of silicate minerals by several orders of magnitude (Fraysse et al., 2009; Iler, 1979). Si_{Am} in soils can be subdivided into Si_{Am} of biogenic origin and of pedogenic origin. The first mainly includes Si in phytoliths, i.e., small bio-opal bodies precipitated in plant tissues that are released during plant-litter decomposition (Barão et al., 2014; Clymans et al., 2015; Schaller et al., 2021). Soil microorganisms (testate amoebae, sponges,
70 diatoms) contribute to less extent (Schaller et al., 2021). Si_{Am} of pedogenic origin, i.e., silica precipitated from soil solution, mainly occurs as soil-particle coatings and void infillings (Schaller et al., 2021). Si_{Am} in topsoils is predominantly of biogenic origin (Clymans et al., 2015; Schaller et al., 2021), whereas Si_{Am} in subsoils is mostly of pedogenic origin (Schaller et al., 2021).

Ecosystem Si cycling can be altered by human impact such as deforestation (Conley et al., 2008), land-use/land-
75 cover (LULC) change (Barão et al., 2020; Struyf et al., 2010), and fire (von der Lühe et al., 2020; Schaller and Puppe, 2021). After LULC transformation from forest to arable land, Si can be lost from the system through harvest, topsoil erosion, and increased soil Si leaching. Soil Si leaching is triggered by reduced interception, which results in increased percolation (Keller et al., 2012; Kraushaar et al., 2021; Vandevenne et al., 2012). Si-

accumulating plants such as rice, wheat, barley, maize, and oil palm (Ma and Takahashi, 2002; Munevar and
Romero, 2015), are characterized by Si accumulation of > 1 wt. % in dry leaf tissue and a Si/Ca ratio > 1 (Ma and
Takahashi, 2002). Such Si accumulators may accelerate Si turnover at the soil-plant interface by taking up high
amounts of Si from soil solution and returning Si-rich litter to soils (Struyf and Conley, 2012, 2009). In oil-palm
plantations, we therefore expected Si losses by harvest and topsoil erosion (Munevar and Romero, 2015;
Vandevenne et al., 2012). In addition, we expected that the spatial arrangement of oil-palms rows and interrows –
with frond piles (frond pile) or without ("empty" interrow) – results in a corresponding spatial Si concentration
pattern in topsoils.

Oil palms are planted in rows (Kotowska et al., 2015) (Fig. 1a). A distance is kept between the rows to ensure
sufficient light exposure (Corley and Tinker, 2016). The space between two oil-palm rows is referred to as an
interrow. They either serve as harvesting paths or as deposition sites for cut-off palm fronds that are stacked up in
long, flat piles (Corley and Tinker, 2016). Fertilizers are only applied within a circle of ~1.5 – 2 m around the
palm stem (palm circle) (Formaglio et al., 2020; Munevar and Romero, 2015). In addition, nutrients are released
from decaying plant litter. Thus, we hypothesized that Si is mainly released and returned to soils in the form of
biogenic Si_{Am} under frond piles, leading to higher topsoil Si_{Am} concentrations, while other management zones
(including palm circles, oil-palm rows and "empty" interrows) might be at risk of Si depletion.

Furthermore, we hypothesized that in oil-palm plantations established on sloping terrain, Si is removed by topsoil
erosion in scarcely vegetated interrows. We assumed that phytoliths might be even more prone to erosion than
mineral soil particles because of their lower density, leading to a disproportionately high Si_{Am} loss through topsoil
erosion. Such additional Si_{Am} loss from interrows would be unfavourable, as interrows may serve as new planting
sites in a subsequent plantation cycle after ~25 years (Corley and Tinker, 2016). Thus, our study aimed at assessing
the impact of management practices in smallholder oil-palm plantations on Si cycling. In addition, we considered
it important to account for potential differences in the intensity of natural desilification in different landscape
positions. Therefore, we carried out the same study in two different landscape positions, associated with differing
water regimes: in well-drained areas with presumably high desilification rates, and riparian areas, where we
assumed that regular flooding might involve an input of Si dissolved in stream water into the system, partially
compensating for desilification.

2 Material and Methods

2.1 Study area and sites

The study was associated to the DFG-funded interdisciplinary Collaborative Research Centre CRC 990, addressing
environmental and socioeconomic impacts of rainforest conversion into plantation systems in Sumatra, Indonesia
(Dislich et al., 2017; Drescher et al., 2016). Thus, it was conducted on CRC 990 plots in smallholder oil-palm
plantations in the Harapan landscape of Jambi Province, Sumatra, Indonesia (1° 55' 0'' S, 103° 15' 0'' E; 50 m ±
5 m NN). Geologically, this lowland landscape is characterised by pre-Paleogene metamorphic and igneous
bedrock that is overlain by lacustrine and fluvial sediments (De Coster, 2006), in which predominantly loamy
mineral soils have formed (Allen et al., 2016). Acrisols were present in well-drained plots, found at higher
elevation and on sloping terrain. Stagnosols and Stagnic Acrisols dominated in seasonally flooded riparian plots,
i.e., in floodplains (Hennings et al., 2021). The Harapan region is characterised by a humid-tropical climate with

a mean annual temperature of 26.7 °C and a mean annual precipitation of 2230 mm (Drescher et al., 2016). The rainy season has two precipitation maxima: one in December and another one in March. A dry period lasts from July to August (Drescher et al., 2016). The natural vegetation is mixed dipterocarp lowland rainforest (Laumonier,

120   1997), which is nearly only preserved in the Harapan rainforest, an ecosystem restoration area in the South of Jambi Province (Harrison and Swinfield, 2015), and in the Barisan mountains in the West of Jambi Province (Drescher et al., 2016). In addition to oil-palm plantations, other important land-use systems in Jambi Province include rubber plantations and agroforestry systems (Dislich et al., 2017).

2.2 Study design and sampling

125   **2.2.1 Topsoil samples**

From April to August 2018, topsoil sampling was conducted in four well-drained (HO1 – HO4) and four riparian plots (HOr1 – HOr4). Oil palms were planted between 1997 and 2001 in well-drained plots, and between 1998 and 2008 in riparian areas (Hennings et al., 2021), following a triangular planting scheme with ~ 9 m distance between the stems (Fig. 1a). Interrows were either used as harvesting paths or to stack cut-off palm fronds (frond

130   pile) (Kotowska et al., 2015). In plot HO1, every interrow contained frond piles. Thus, topsoil samples of interrows were obtained only from three well-drained plots. The understory vegetation of all well-drained plots was occasionally weeded. Two riparian plots (HOr1 and HOr2) had a well-maintained grass cover between the oil palms.

In each of the eight plots, topsoil samples were taken with steel cylinders (height = 4 cm, volume = 100 cm³) at

135   five locations along the slope. At each location, topsoils were sampled from four different management zones, i.e., (1) palm circle, (2) oil-palm row, (3) interrow, and (4) frond pile, to assess spatial patterns of Si_{Am} and Si_M concentrations in topsoils within the oil-palm plantations (Appendix, Table A1 and A2). Interrow topsoil samples were taken at a maximum distance between oil palms. The samples were dried (40 °C, 24 h) and sieved (≤ 2 mm) prior to Si analyses. An aliquot of each sample was dried at 105 °C to determine the water content of the samples

140   dried at 40 °C.

2.2.2 Sediment traps

Sediment traps were installed in sets of two in interrows of the well-drained plots HO1 – HO4, on 8 – 12° sloping land (Sinukaban et al., 2000). Each trap consisted of a rectangular aluminium frame (2 x 1 m, 2 m²). Its downslope-facing short side was funnel-shaped, directing surface runoff and eroded soil material into a bucket (Fig. 1b and

145   Appendix, Table A3). A second bucket was connected to the first bucket by a 2 cm thick tube to catch potential overflow. The traps were checked and maintained weekly from the beginning of September 2018 to the end of August 2019. The understory vegetation in the sediment traps was kept in place to ensure that the understory vegetation was representative of the oil-palm plantations. Both sediment traps in HO1 were manually weeded after six months because inside the traps, vegetation covered nearly 100 % of the soil surface, impeding topsoil erosion.

150   Eroded soil material was collected whenever present, dried (40 °C, 48 h), sieved (≤ 2 mm) and weighed prior to Si analyses. Samples of eroded soil material from plot HO2 were excluded from further analysis because both traps got contaminated by crude oil. Losses of Si_{Am} were calculated for each sediment trap by multiplying the concentration of Si_{Am} of each sediment sample by the amount of eroded soil material collected by each trap (Appendix, Table B2). Erosion estimates were determined for each trap by summing up the amount of eroded soil

155 material for the 12-months period from the beginning of September 2018 until the end of August 2019. Precipitation data of the two closest meteorological stations were used for correlating the observed soil erosion with precipitation. Distances between meteorological stations and plots comprised ~ 2 km for HO1, ~ 3 km for HO2, ~ 8 km for HO3, and ~ 6 km for HO4. At each meteorological station, precipitation was measured by two automated precipitation transmitters (Thies Clima, Göttingen, Germany), at a height of 1.5 m and a horizontal

160 distance of about 6 m.
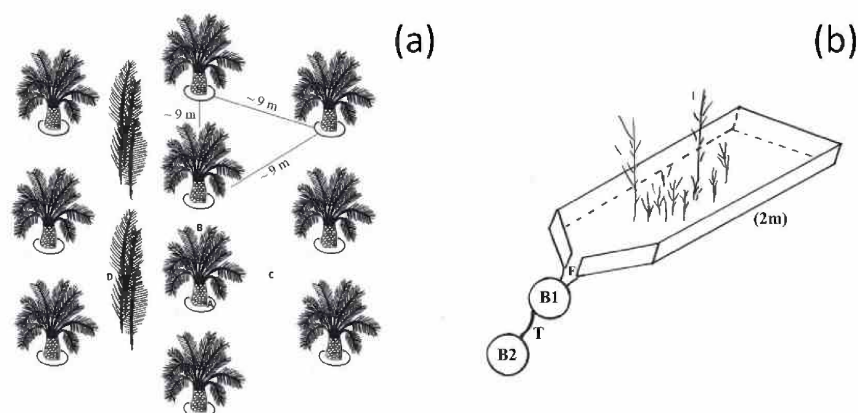
Figure 1a Triangular planting arrangement on smallholder oil-palm plantations in the study area (sketch by B. Greenshields). Topsoil samples were taken in four distinct management zones: (A) in palm circles. (B) in oil-palm rows, (C) in interrows and (D) below frond piles.

Figure 1b 2 m² sediment trap with scarce understorey vegetation as installed in pairs in four well-drained plots (sketch by B. Greenshields after S. Tarigan). The downslope funnel-shaped part of the aluminium frame (F) directs surface runoff, together with eroded soil material, into a bucket (B1) that is connected to a second bucket (B2) by a 2 cm wide tube (T). Photos of the sediment traps are shown in the Appendix, Table A3.

2.3 Determination of silicon pools in topsoils

2.3.1 Silicon in amorphous silica (Si_{Am})

Si_{Am} was extracted from topsoil samples and eroded soil material by 1 % Na_2CO_3 solution (Meunier et al., 2014). At 85 °C, amorphous silica dissolves within 2 – 3 hours in 1 % Na_2CO_3 solution, thereby rapidly raising the Si

165 concentration in solution. Once amorphous silica is completely dissolved, the release of Si to solution is only sustained by the slower dissolution of silicate minerals which follows a linear trend. Si concentration was measured four times during the linear dissolution phase. A linear equation was fitted to the data. The Si_{Am} concentration was inferred from the y-intercept of the linear regression.

In detail, 40 ml of 1 % Na_2CO_3 solution were added to approximately 30 mg of soil material. The samples were

170 then placed into a shaking water bath at 85 °C. To ensure steady Si release from topsoils, the samples were manually shaken at time intervals of 45 min. Aliquots were taken after 3 h, 3.75 h, 4.5 h, and 5.25 h. For this purpose, the samples were taken out of the water bath, cooled in a cold-water basin (10 min) and centrifuged (5

min, 3000 rpm). A 0.25 ml aliquot was taken from the supernatant of each sample and neutralized with 2.25 ml
0.021 M HCl. Si concentrations in the aliquots were analysed by the molybdenum blue method (Grasshoff et al.,
175   2009) using a UV-VIS spectrophotometer (Lamda 40, Perkin Elmer, Germany) at 810 nm. We chose 1 % Na_2CO_3
as an extractant and used the extraction method by Meunier et al. (2014) instead of the stronger extractant 0.1 M
NaOH used by Barão et al. (2015) because we assumed that most Si in topsoils is of biogenic origin and dissolved
well by Na_2CO_3 (Meunier et al., 2014).

2.3.2 Mobile silicon (Si_M)

180   Si_M was extracted by $CaCl_2$ solution, which provides electrolytes resembling natural soil solutions (Georgiadis et
al., 2013; Sauer et al., 2006). From each sample, 1 g of soil material was mixed with 5 ml of 0.01 M $CaCl_2$ and
left for 24 h, shaking for 1 min h^{-1} on an overhead shaker. Samples were centrifuged (5 min, 3000 rpm) and the
supernatant was filtered through ash-free paper filters (1-2 μm). Si concentrations were analysed in filtrates by the
molybdenum blue method. We transformed the measured Si concentration (μg g^{-1}) into the amount of Si_M per
185   gram 105 °C dried soil.

2.4 Statistical analyses

Statistical analyses were conducted on the grand means of topsoil Si concentrations in each water regime and
management zone. The two latter were grouped into (i) palm circles in well-drained / riparian areas (each, n = 4),
(ii) oil-palm rows in well-drained / riparian areas (each, n = 4), (iii) interrows in well-drained (n = 3) / riparian
190   areas (n = 4) and (iv) frond piles in well-drained / riparian areas (each, n = 4). The four management zones were
tested for significant differences in topsoil Si concentrations, both within the well-drained and within the riparian
areas. In addition, we tested the well-drained and riparian areas for significant differences in topsoil Si
concentrations by comparing the same management zone under two different water regimes. The data was log
transformed to assert normal distribution (Shapiro-Wilk test) and homogeneity of variances (Levene test). Both
195   criteria were met for all groups except for Si_M in topsoils of oil-palm rows in well-drained areas (Appendix, Table
B3). We conducted a one-way analysis of variance (ANOVA) to detect if Si_{Am} and Si_M concentrations in topsoils
of different management zones differed significantly within well-drained and within riparian areas, as well as
between well-drained and riparian areas. Then we used the Tuckey-Kramer post-hoc test to identify, which
management zones differed significantly. The level of significance was set at $p \leq 0.05$. We used the open-source
200   software R version 3.6.2 and R CRAN packages ggplot2, ggpubr, car and psych to perform these statistical
analyses.

3 Results

3.1 Concentrations of Si_{Am} and Si_M in topsoils

In well-drained plots, mean topsoil Si_{Am} concentrations were about twice as high under frond piles (3.97 ± 0.76
205   mg g^{-1}) compared to palm circles (1.71 ± 0.36 mg g^{-1}), oil-palm rows (1.87 ± 0.28 mg g^{-1}) and interrows (1.88 ±
0.32 mg g^{-1}) (Fig. 2a). This difference between frond piles and the other three management zones was significant
($p \leq 0.05$) (Fig. 2a). In riparian plots, mean topsoil Si_{Am} concentrations were equally high below frond piles (2.96
± 0.36 mg g^{-1}) and in interrows (2.71 ± 0.13 mg g^{-1}) (Fig. 2b). Compared to these two management zones, mean
topsoil Si_{Am} concentrations in palm circles (1.44 ± 0.30 mg g^{-1}) were significantly lower ($p \leq 0.05$) (Fig. 2b). Oil-

210   palm rows had intermediate mean topsoil Si_{Am} concentrations (2.08 ± 0.63 mg g^{-1}) (Fig. 2b), showing no significant difference with respect to any other management zone ($p \leq 0.05$).

In well-drained plots, mean topsoil Si_M concentrations were about twice as high under frond piles (13.68 ± 6.54 µg g^{-1}) and in palm circles (11.17 ± 5.42 µg g^{-1}) compared to oil-palm rows (6.38 ± 2.85 µg g^{-1}) and interrows (5.62 ± 0.10 µg g^{-1}) (Fig. 2c). Only plot HO1 showed exceptionally high topsoil Si_M concentrations in oil-palm

215   rows (outlier), which could be attributed to the dense vegetation throughout that smallholder plantation. In riparian plots, mean topsoil Si_M concentrations were twice as high under frond piles (19.56 ± 6.13 µg g^{-1}) compared to mean topsoil Si_M concentrations in palm circles, oil-palm rows and interrows, the latter all ranging around 11 µg g^{-1} (Fig. 2d). Mean topsoil Si_M concentrations did not differ significantly ($p \leq 0.05$) between the other management zones within the same water regime (well-drained/riparian), nor did mean topsoil Si_M concentrations (in the same

220   management zone) differ between water regimes.
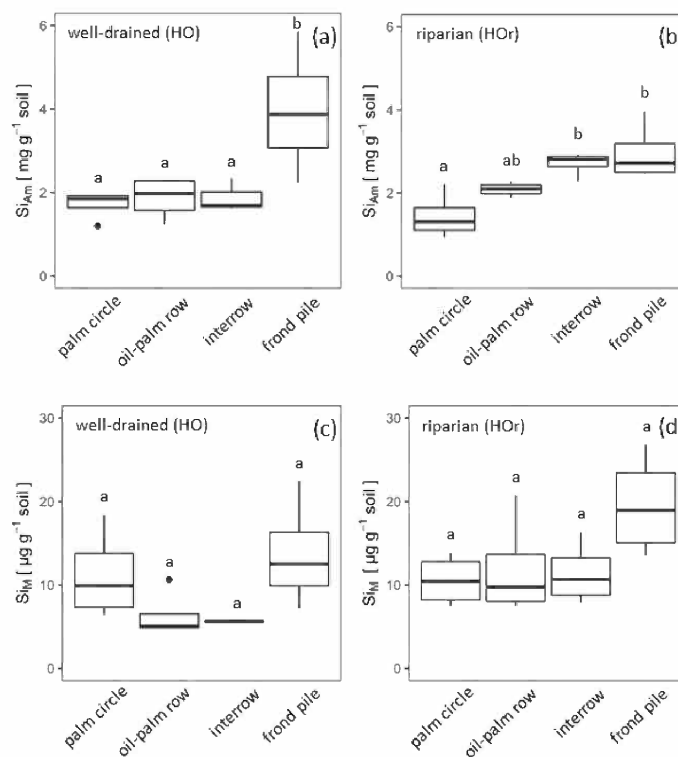
Figure 2 Concentrations of mobile Si (Si_M) and Si in amorphous silica (Si_{Am}) in topsoils of four different management zones: palm circles (n = 4), oil-palm rows (n = 4), interrows (n = 3), and under frond piles (n = 4) on smallholder oil-palm plantations in two different landscape positions with differing water regimes (well-drained and riparian). Boxes indicate interquartile ranges and whiskers extend 1.5 times the interquartile range below or above the box. Lower case letters indicate significant differences between management zones within a water regime ($p \leq 0.05$). calculated with one-way analysis of variance (ANOVA) and Tukey-Kramer post-hoc test.

3.2 Topsoil erosion and associated losses of Si_{Am}

In plots HO3 and HO4, median Si_{Am} concentrations in topsoils of interrows (1.53 – 1.57 mg g^{-1}) were roughly twice as high as in eroded soil material (0.66 – 0.88 mg g^{-1}) (Tab. 1). In plot HO1, the median Si_{Am} concentration in eroded soil material (1.61 mg g^{-1}) was twice as high as in eroded soil material of plots HO3 and HO4 (0.66 – 0.88 mg g^{-1}). Over the entire sampling period of 12 months, the four sediment traps in plots HO1 and HO4 indicated erosion rates of ~ 4 – 5 Mg ha^{-1} yr^{-1} (Tab. 2). In plot HO3, a similar erosion rate was obtained from trap 1 (~ 6 Mg ha^{-1} yr^{-1}), whereas the erosion rate observed in trap 2 of plot HO3 was twice as high (~ 12 Mg ha^{-1} yr^{-1}). Si_{Am} losses through topsoil erosion amounted to 6 – 9 kg ha^{-1} yr^{-1} in the four sediment traps of HO1 and HO3, and 5 – 7 kg ha^{-1} yr^{-1} in both sediment traps of HO4. Figure 3 presents weekly losses of topsoil and Si_{Am} in eroded topsoil correlated with daily rainfalls. During the 12-month sampling period, daily rainfalls ≥ 25 mm d^{-1} were recorded from mid-September 2018 until mid-June 2019 (Fig. 3). The rainy season started in November 2018 with daily rainfalls exceeding 60 mm d^{-1} (HO4, weather station near a state-owned plantation) to 70 mm d^{-1} (HO1 and HO3, weather station near the village of Bungku) after a dry spell in October. A second rainy peak lasted from mid-March to mid-April 2019 with daily rainfalls reaching 50 mm d^{-1} (HO1 and HO3) to 70 mm d^{-1} (HO4). The dry season started in mid-June 2019, showing only one intense rainfall event (outlier, HO4) at the end of August 2019.

In plot HO1, a dense cover of mosses, grasses, and 20 – 50 cm high understorey vegetation prevented soil loss from September 2018 until end of January 2019. (Tab. 1, Fig. 3a). After manually weeding plot HO1 at the end of January 2019, the vegetation coverage was kept minimal (around 5 %). Noticeable losses of soil and corresponding losses of Si_{Am} occurred between February (13 – 21 g m² of sediment, 16 – 53 mg m² of Si_{Am}) and the end of May 2019 (16 – 100 g m² of sediment / 38 – 192 mg m² of Si_{Am}) (Fig. 3a and 3b). In plot HO3, scare understorey vegetation of herbaceous plants (no grasses and mosses) covered about a third of the sediment traps (Tab. 1). Soil and corresponding Si_{Am} losses were recorded continuously from September 2018 to May 2019 (Fig. 3.3). Each week, losses of topsoil material amounted to 4 – 62 g m² (corresponding to 1 – 90 mg m² Si_{Am}) (Fig. 3a, 3b). At three sampling dates, one in December 2018 and two in February 2019, peak soil losses ≥ 150 g m² occurred. The corresponding Si_{Am} losses of these sampling dates were ≥ 90 mg m², hence also representing among the highest Si_{Am} losses throughout the sampling period. In plot HO4, vegetation coverage in the traps increased from 40 % in September 2018 to 60 % in May 2019 (Tab. 1). Soil loss occurred from mid-September 2018 to the end of May 2019 (Fig. 3). Losses of eroded soil material barely exceeded 50 g m² of sediment. However, an event with approximately 20 g m² of soil loss had corresponding Si_{Am} losses ranging from 5 – 160 mg m², thus showing a large variability.

Table 1 Topsoil Si_{Am} concentrations in interrow and sediment trap samples

Oil-palm plot	N^c	Statistics	Interrow Si_{Am} [mg g^{-1}$_{soil}$]	Eroded soil material Si_{Am} [mg g^{-1}$_{soil}$]	Estimated vegetation cover (Sep / Jan / Apr-May [%])
HO1[a]	NA/19	MIN	NA[d]	0,90	100 / 5 / 5
HO1[a]	NA/19	MEDIAN	NA[d]	**1,61**	
HO1[a]	NA/19	MEAN	NA[d]	1,77	
HO1[a]	NA/19	MAX	NA[d]	3,26	
HO3[b]	5/38	MIN	1,40	0,11	30 / 40 / 30
HO3[b]	5/38	MEDIAN	**1,53**	**0,88**	
HO3[b]	5/38	MEAN	1,63	0,82	
HO3[b]	5/38	MAX	1,91	1,97	
HO4[b]	5/27	MIN	1,45	0,03	40 / 50 / 60
HO4[b]	5/27	MEDIAN	**1,57**	**0,66**	
HO4[b]	5/27	MEAN	1,69	1,13	
HO4[b]	5/27	MAX	2,21	6,84	

[a] Si_{Am} concentrations for plot HO1 as of February 2019 (after manual weeding)
[b] Si_{Am} concentrations for plot HO3 and HO4 for the whole sampling duration
[c] replicates for interrow topsoil samples/replicates for eroded soil samples
[d] every interrow on plot HO1 contained stacked frond piles, no sampling possible

Table 2 Annual losses of soil and Si_{Am} through erosion

Plot	Trap	Eroded soil material [Mg soil ha^{-1} yr^{-1}]	Si_{Am} [kg Si_{Am} ha^{-1} yr^{-1}]
HO1	1	5.4	8.7
HO1	2	4.2	7.2
HO3	1	11.7	8.9
HO3	2	6.1	6.0
HO4	1	5.4	6.7
HO4	2	3.6	4.6
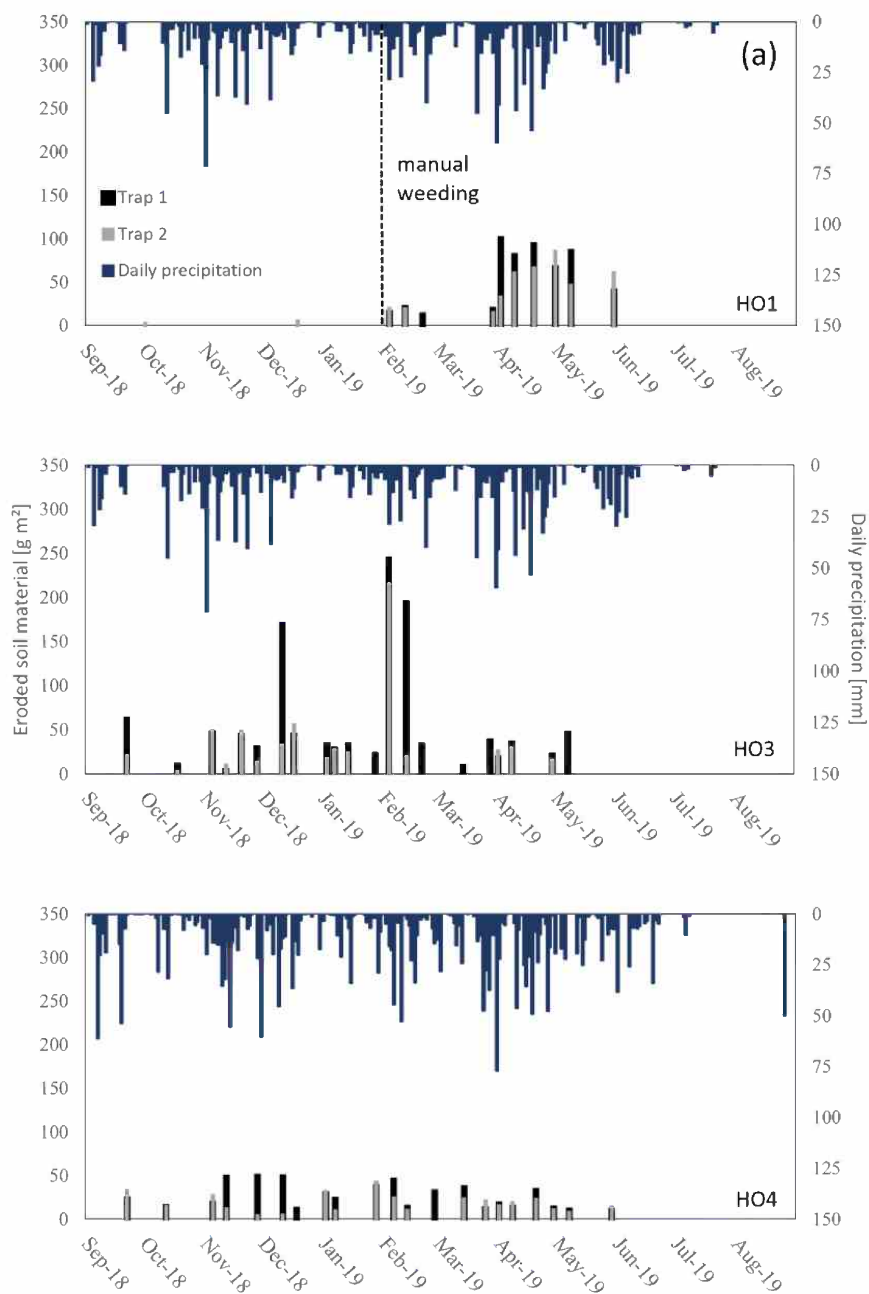
Figure 3a Weekly losses of topsoil, collected from sediment traps (n = 6) of oil-palm plantations in well-drained areas.
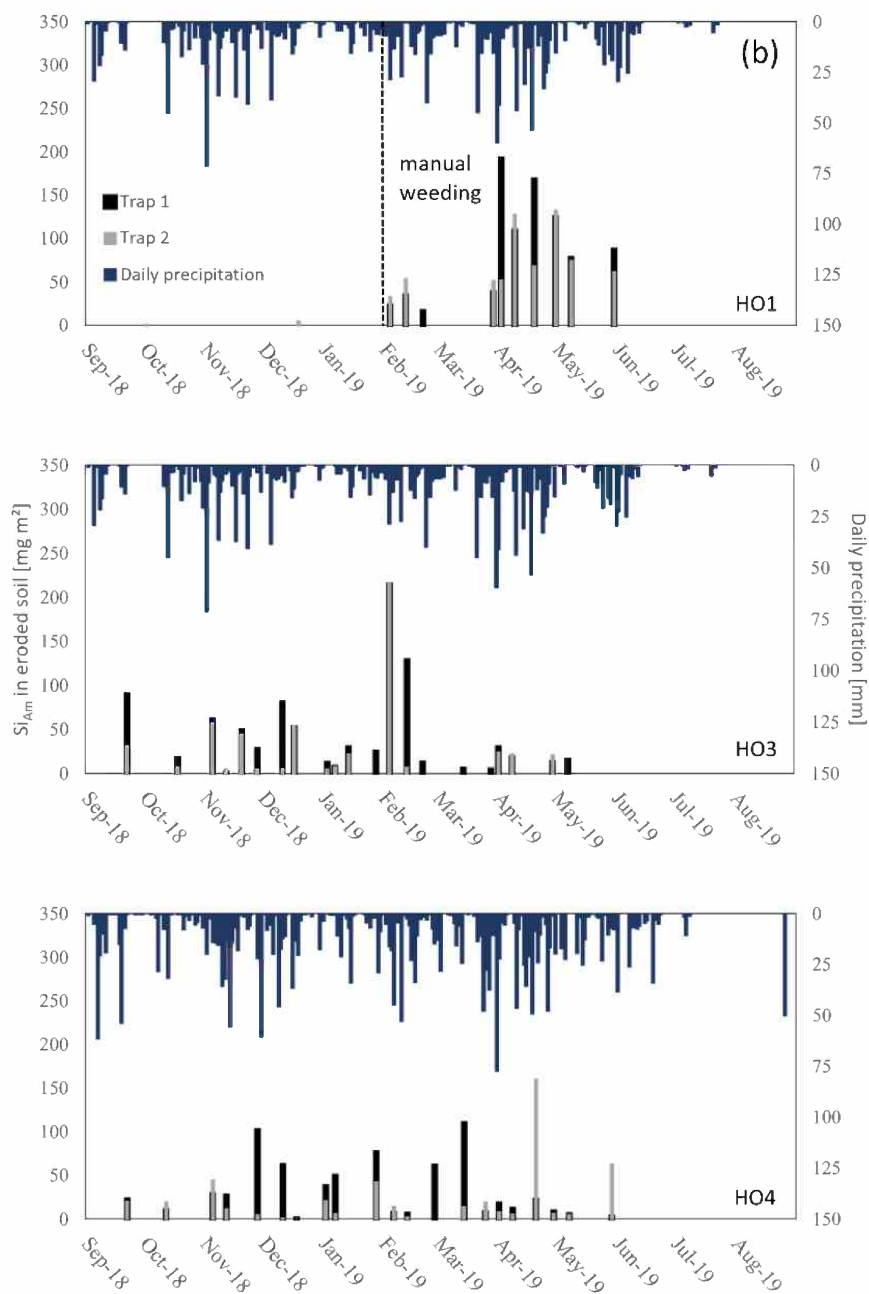
Figure 3b Weekly losses of Si in amorphous silica (Si_{Am}) in eroded topsoil, collected from sediment traps (n = 6) of oil-palm plantations in well-drained areas.

255

4 Discussion

4.1 Spatial topsoil Si_{Am} concentration patterns

In oil-palm plantations, cut-off palm fronds stacked in every second interrow represent the main source of phytoliths (Albert et al., 2015; Clymans et al., 2015; Huisman et al., 2018) although these frond pile areas may occupy less than 15 % of plantation area (Tarigan et al., 2020). Once phytoliths are released into topsoils, they can replenish the topsoil Si_{Am} pool. Therefore, we had hypothesized that Si_{Am} is mainly returned to soils under frond piles (cf. section 1), leading to a spatial topsoil Si_{Am} pattern with higher Si_{Am} concentrations under frond piles. This hypothesis was corroborated for well-drained plots as topsoil Si_{Am} concentrations were indeed significantly higher (2-fold) under frond piles ($\sim$4 mg g^{-1}) than in all other management zones ($\sim$2 mg g^{-1}) (Fig. 2a). Lower Si_{Am} levels in palm circles, oil-palm rows and interrows may reflect the pedogenic Si_{Am} pool with only minor contributions of biogenic Si_{Am}, e.g., from grass phytoliths. A possible reason for this is that decaying palm fronds are not returned to these management zones.

In the riparian plots, topsoil Si_{Am} concentrations were equally high under frond piles and in interrows ($\sim$ 3 mg g^{-1}). This can only be explained by an additional important source of topsoil Si_{Am} in interrows that was present in the riparian plots. The only potential Si_{Am} source includes litter of grasses (*Poaceae*) and sedges (*Cyperaceae*) which also releases considerable amounts of phytoliths upon its decomposition. Grasses and sedges are considered effective Si accumulators, too (Blecker et al., 2006; Quigley et al., 2017). This explanation is further supported by the significantly lower ($p \leq 0.05$) topsoil Si_{Am} concentrations in palm circles ($\sim$1.4 mg g^{-1}) (Fig. 2b). Palm circles are weeded and treated with herbicides regularly. Thus, this management zone also lacks litter return and with that a principal source of Si. The significant difference in topsoil Si_{Am} concentrations between interrows and palm circles can only be explained by the presence or absence of grasses as phytolith sources. This observation highlights the importance of grasses and sedges in oil-palm plantations as they can also maintain soil-plant-Si cycling in the system. Thus, our original hypothesis that Si_{Am} is mainly returned to the soils under frond piles, while topsoils in other management zones tend to be depleted in Si_{Am}, is valid only in oil-palm plantations with a negligible grass cover.

The absence of any significant differences in topsoil Si_{Am} concentrations between the two differing water regimes suggests that there was no noticeable Si supply by stream water to topsoils in riparian areas. In fact, release rates of biogenic Si_{Am} from decaying oil-palm and other litter must be similar in both water regimes, likewise, the rate at which oil palms take up Si from soil solution or form phytoliths.

4.2 Si_{Am} losses through topsoil erosion

Corley & Tinker (2016) summarized some early works by Kee and Chew (1996) and Maene et al. (1979) estimating soil-erosion rates under oil-palm plantations. They reported losses of ≤ 9 Mg ha^{-1} yr^{-1} from sloping oil-palm plantations on Plinthic Acrisols and Haplic Nitisols in Malaysia (Arshad, 2015; Corley and Tinker, 2016). In our study we obtained soil losses of $\sim 4 - 6$ Mg ha^{-1} yr^{-1}. This puts our estimates into a comparable range (except for trap 1 in plot HO3 that yielded ~ 12 Mg ha^{-1} yr^{-1}). However, short-term experiments can easily overestimate soil erosion rates, if upscaled to landscape level (Breuning-Madsen et al., 2017). The observations by Breuning-Madsen et al. (2017) would imply that the soil losses we obtained for oil-palm plantations are ~ 2 orders of magnitude higher than in a secondary forest (Breuning-Madsen et al., 2017). Considerable erosion (soil loss of $\sim$

35 cm during a 15-year cultivation period, which corresponds to ~ 28 Mg ha^{-1} yr^{-1}) was noted by Guillaume et al. (2015), who compared δ^{13}C values in soil profiles on the same well-drained oil-palm plantations of our study region. High erosion rates are to be expected, as oil-palm plantations have a rather open canopy compared to rainforests, permitting rain drops to directly hit the ground (Corley and Tinker, 2016; Oliveira et al., 2013).

During heavy rainfalls, rain drops release kinetic energy that breaks up soil aggregates, especially when hitting bare soil. Mobilized fine and broken aggregates can fill soil pores thereby reducing infiltration, promoting surface run-off (Oliveira et al., 2013; Tarigan et al., 2020) and hence erosion. Besides, soil compaction may be substantial in oil-palm interrows, which are frequently used as harvesting paths and are therefore kept vegetation-free, which makes them particularly prone to surface runoff and erosion (Comte et al., 2012; Guillaume et al., 2016). This explanation is further supported by our sediment trap data: traps with a low vegetation cover (e.g., HO3 whole year and HO1 as of February 2019) exposed to daily rainfalls exceeding 25 mm d^{-1} showed higher losses of soil (~ 50 – 100 g m², Tab 1. and Fig. 3a) than traps (e.g., HO4 whole year and HO1 prior to February 2019) that had less than 50 % of bare soil at similar rainfall intensities. This again highlights the importance of cover crop in oil-palm plantations countering soil erosion (Corley and Tinker, 2016; Guillaume et al., 2015, 2016; Luke et al., 2019). Furthermore, stacked palm fronds, especially if aligned perpendicular to the slope, may reduce soil erosion on oil-palm plantations (Corley and Tinker, 2016).

One of the questions to be answered in this study was, to what extent soil erosion reduces the topsoil Si$_{Am}$ pool in oil-palm plantations, and whether the lower density of phytoliths compared to mineral soil particles caused proportionally greater losses of Si$_{Am}$ through soil erosion. To our knowledge, only a few studies exist, in which the effect of soil erosion on the topsoil Si$_{Am}$ pool has been addressed. Almost all of them focused on arable soils (Clymans et al., 2015; Kraushaar et al., 2021; Unzué-Belmonte et al., 2017). Clymans et al. (2015) determined mean topsoil Si$_{Am}$ concentrations of 1.76 mg^{-1} g^{-1} in arable fields in sloping terrain and temperate climate. This compares well to topsoil Si$_{Am}$ concentrations in interrows from our study (Tab. 1). In contrast, Si$_{Am}$ concentrations in eroded soil material differed by factor two between plots HO1 (1.61 mg g^{-1}) towards HO3 (0.88 mg g^{-1}) and HO4 (0.66 mg g^{-1}) (Tab 1 and Appendix, Table B2). A possible explanation could be the differing maintenance of the cover crop. High median Si$_{Am}$ concentrations in eroded soil material were determined in previously vegetated traps (e.g., HO1 until the end of January 2019), whereas lower median Si$_{Am}$ concentrations in eroded soil material were measured in traps with less vegetation (HO3 and HO4, whole year, Tab. 1). We may infer from this observation that the cover crop in plot HO1 maintained higher Si levels in the topsoil through continuous phytolith release from litter. After weeding and keeping the vegetation cover at around 5 %, this phytolith-enriched topsoil was eroded leading to higher Si$_{Am}$ concentrations in the eroded soil material. In contrast, plots HO3 and HO4 had lower, and more dispersed Si$_{Am}$ concentrations in eroded soil material as they lacked an additional Si source. Further, low Si$_{Am}$ concentrations suggest that topsoil with originally high amounts of biogenic Si$_{Am}$ has already been eroded over time, leaving mainly pedogenic Si$_{Am}$. A greater variability in Si$_{Am}$ concentrations in eroded soil material in plots HO3 and HO4 was probably caused by a slight increase in vegetation cover during the year and secondarily, by varying daily rainfalls (Fig. 3). Thus, these observations could provide a basis to state that phytoliths are preferably eroded from topsoils. This in turn would assert our hypothesis. Nevertheless, further field experiments and observations are required to confirm this statement.

4.3 Spatial topsoil Si_M concentration patterns

Topsoil Si_M concentrations in well-drained plots were highest under frond piles (~14 µg g^{-1}), followed by palm circles (~11 µg g^{-1}), and lowest in oil-palm rows and interrows (~6 µg g^{-1}). However, these differences were not
335   statistically significant (Fig. 2c, 2d). Higher topsoil Si_M concentrations under frond piles can be explained by the high solubility of Si_{Am} that is released from decaying palm fronds in the form of phytoliths. In addition to Si_{Am} (Barão et al., 2014; Unzué-Belmonte et al., 2017), Si associated to soil organic matter (SOM) also represents a readily soluble Si fraction in topsoils (Alexandre et al., 1997; Georgiadis et al., 2013; von der Lühe et al., 2020). Such readily soluble Si fractions usually contribute most Si to soil solution (Struyf et al., 2010; de Tombeur et al.,
340   2020).

The plots in the riparian areas showed high topsoil Si_M concentrations under the frond piles (~20 µg g^{-1}). All other management zones had lower topsoil Si_M concentrations in the range of ~11 – 12 µg g^{-1} (Fig. 2b). However, this difference was also not statistically significant. In riparian plots, flooding may lead to a redistribution of Si_M across the oil-palm plantation, hence explaining similar topsoil Si_M concentrations in palm circles, oil-palm rows and
345   interrows. In riparian areas that are flooded during the rainy season, dissolved Si in stream water (Cornelis et al., 2011; Dürr et al., 2011) may be another source of topsoil Si_M alongside Si_{Am}. Therefore, we had hypothesised that Si input from stream water may lead to higher topsoil Si_M levels in riparian areas compared to well-drained areas. Indeed, topsoil Si_M concentrations under frond piles in riparian plots (~20 µg g^{-1}) tended to be higher compared to well-drained plots (~14 µg g^{-1}). Likewise, topsoil Si_M concentrations in oil-palm rows and interrows in riparian
350   plots (~11-12 µg g^{-1}) also tended to be higher compared to well-drained plots (~6 µg g^{-1}). However, these differences were not statistically significant so our hypothesis cannot be fully asserted.

5 Conclusions and recommended measures

Based on the differing topsoil Si_{Am} concentrations observed in the different management zones, we conclude that current oil-palm management practices cause a distinct spatial topsoil Si_{Am} concentration pattern. Especially the
355   stacking of cut-off palm frond in long piles and subsequent decomposition promotes Si_{Am} return to soils. Thus, highest topsoil Si_{Am} concentrations occur below frond piles. Similarly, high concentrations may be found in interrows, if additional sources of biogenic Si_{Am} such as Si-accumulating plants (grasses, sedges) are present. Lower topsoil Si_{Am} concentrations in oil-palm rows and unvegetated interrows reflect a lack of Si_{Am} return to soils through plant litter in these management zones. Moreover, pronounced topsoil erosion in unvegetated interrows
360   involves Si_{Am} losses and may therefore cause additional Si_{Am} depletion in this management zone. A dense cover of grasses and mosses in interrows may efficiently reduce erosion and associated Si_{Am} losses.

Topsoil Si_M concentrations in the different management zones showed that biogenic Si_{Am} was an important readily available source of Si_M. Thus, analogous to topsoil Si_{Am} concentrations, highest topsoil Si_M concentrations also occurred under frond piles. Our hypothesis that regular flooding involves an input of Si dissolved in stream water
365   into the system in riparian areas, partially replenishing the Si_M pool, could not be statistically proven in this study. Although topsoil Si_M concentrations tended to be higher in riparian areas, the differences between well-drained and riparian plots were not statistically significant.

In conclusion, our findings suggest that erosion could be reduced efficiently, and Si cycling could be maintained within the system if smallholders followed some suggested measures such as (1) maintaining the cover crop in oil-

370 palm rows and interrows, (2), incorporating oil-palm litter into farm management and (3) preventing soil compaction and surface-crust formation.

6 Appendix

Table A1 Representative elevation transects of topsoil sampling under oil-palm plantations

Plot	GPS position 1		GPS position 2		Elevation [m]
HO1	S 01° 54.583'	E 103° 15.996'	S 01° 54.587'	E 103° 16.015'	85
HO2	S 01° 53.012'	E 103° 16.017'	S 01° 52.987'	E 103° 16.018'	76
HO3	S 01° 51.442'	E 103° 18.490'	S 01° 51.445'	E 103° 18.522'	25
HO4	S 01° 47.188'	E 103° 16.246'	S 01° 47.195'	E 103° 16.229'	60
HOr1	S 01° 54.107'	E 103° 22.887'	S 01° 54.124'	E 103° 22.993'	28
HOr2	***	***	***	***	***
HOr3	S 01° 51.662'	E 103° 18.357'	S 01° 51.656'	E 103° 18.383'	48
HOr4	S 01° 42.687'	E 103° 17.544'	S 01° 42.666'	E 103° 17.536'	33

Table A2 Topsoil sampling, fieldwork 2018

HO1 – oil-palm row   HO1 – oil-palm row (detailed view)

375

Table A3 Sediment traps in interrows of well-drained oil-palm plantations.

HO1 – September 2018	HO1 – February 2019	HO1 – May 2019
HO3 – September 2018	HO3 – January 2019	HO3 – April 2019

HO4 – September 2018   HO4 – January 2019   HO4 – May 2019

Well-drained – Interrow   Riparian – Interrow

Table B1 Topsoil Si concentrations in different management zones of oil-palm plantations

Management zone	Plot	Water regime	Si_{Am} [mg g^{-1}$_{soil}$]		Si_M [μg g^{-1}$_{soil}$]	
			$\bar{x}$ ± σ		$\bar{x}$ ± σ	
Palm circle	HO1	Well-drained	1,93 ± 0,25		12,23 ± 4,83	
Palm circle	HO2	Well-drained	1,92 ± 0,70		7,61 ± 4,13	
Palm circle	HO3	Well-drained	1,78 ± 1,08		18,38 ± 5,47	
Palm circle	HO4	Well-drained	1,20 ± 0,43		6,45 ± 3,10	
Oil-palm row	HO1	Well-drained	2,27 ± 0,93		10,65 ± 1,96	
Oil-palm row	HO2	Well-drained	2,28 ± 0,31		5,17 ± 1,15	
Oil-palm row	HO3	Well-drained	1,23 ± 0,54		4,77 ± 0,49	
Oil-palm row	HO4	Well-drained	1,68 ± 0,35		4,94 ± 0,83	
Interrow	HO1	Well-drained	*** ±		*** ±	
Interrow	HO2	Well-drained	2,34 ± 0,81		5,52 ± 1,16	
Interrow	HO3	Well-drained	1,63 ± 0,21		5,72 ± 1,56	
Interrow	HO4	Well-drained	1,69 ± 0,30		5,64 ± 2,39	
Frond pile	HO1	Well-drained	4,42 ± 1,47		22,47 ± 10,7	
Frond pile	HO2	Well-drained	5,86 ± 2,25		10,81 ± 2,37	
Frond pile	HO3	Well-drained	3,35 ± 0,92		14,26 ± 4,03	
Frond pile	HO4	Well-drained	2,24 ± 0,50		7,18 ± 1,50	
Palm circle	HOr1	Riparian	0,94 ± 1,02		8,46 ± 2,54	
Palm circle	HOr2	Riparian	2,21 ± 0,62		12,44 ± 1,55	
Palm circle	HOr3	Riparian	1,46 ± 0,46		7,49 ± 2,34	
Palm circle	HOr4	Riparian	1,16 ± 0,33		13,82 ± 1,56	
Oil-palm row	HOr1	Riparian	2,27 ± 1,62		8,23 ± 4,78	
Oil-palm row	HOr2	Riparian	2,02 ± 0,54		20,74 ± 3,48	
Oil-palm row	HOr3	Riparian	1,88 ± 0,20		7,50 ± 0,97	
Oil-palm row	HOr4	Riparian	2,17 ± 0,42		11,30 ± 0,42	
Interrow	HOr1	Riparian	2,29 ± 0,64		9,07 ± 2,67	
Interrow	HOr2	Riparian	2,86 ± 0,69		16,26 ± 2,50	
Interrow	HOr3	Riparian	2,76 ± 0,46		7,92 ± 1,03	
Interrow	HOr4	Riparian	2,93 ± 0,76		12,26 ± 2,49	
Frond pile	HOr1	Riparian	2,51 ± 0,81		13,53 ± 4,70	
Frond pile	HOr2	Riparian	2,46 ± 1,51		26,83 ± 2,71	
Frond pile	HOr3	Riparian	3,95 ± 1,24		15,57 ± 4,63	
Frond pile	HOr4	Riparian	2,93 ± 0,77		22,30 ± 11,1	

380

Table B2 Weekly loss of eroded soil material and Si_{Am} in eroded soil material from sediments traps under oil-palm plantations (sloping terrain)

Date	Month	Trap	Plot	Si_{Am} [mg g^{-1} soil] $\bar{x}$ ± σ	Eroded soil material [g per 2m² trap]	Si_{Am} in eroded soil material [mg per 2m² trap]	Eroded soil material [g m²]	Si_{Am} in eroded soil material [mg m²]
2018-10-02	October	HO1_2	HO1	0,21 ± 0,03	5,59	1,18	2,80	0,6
2018-12-19	December	HO1_2	HO1	0,79 ± 0,07	11,67	9,23	5,84	4,6
2019-02-04	February	HO1_1	HO1	1,48 ± 0,18	30,83	45,56	15,42	22,8
2019-02-04	February	HO1_2	HO1	1,59 ± 0,07	41,10	65,29	20,55	32,6
2019-02-12	February	HO1_1	HO1	1,61 ± 0,26	42,08	67,90	21,04	34,0
2019-02-12	February	HO1_2	HO1	2,66 ± 0,29	39,92	106,11	19,96	53,1
2019-02-21	February	HO1_1	HO1	1,28 ± 0,05	25,26	32,42	12,63	16,2
2019-03-29	March	HO1_1	HO1	1,99 ± 0,04	37,83	75,23	18,92	37,6
2019-03-29	March	HO1_2	HO1	3,26 ± 0,04	31,40	102,33	15,70	51,2
2019-04-02	April	HO1_1	HO1	1,92 ± 0,11	200,29	383,69	100,15	191,8
2019-04-02	April	HO1_2	HO1	1,53 ± 0,28	67,23	103,14	33,62	51,6
2019-04-09	April	HO1_1	HO1	1,35 ± 0,02	161,75	218,07	80,88	109,0
2019-04-09	April	HO1_2	HO1	2,10 ± 0,49	121,74	255,20	60,87	127,6
2019-04-19	April	HO1_1	HO1	1,80 ± 0,23	186,72	336,06	93,36	168,0
2019-04-19	April	HO1_2	HO1	1,01 ± 0,04	134,16	135,93	67,08	68,0
2019-04-30	April	HO1_1	HO1	1,87 ± 0,24	133,01	248,75	66,51	124,4
2019-04-30	April	HO1_2	HO1	1,53 ± 0,19	172,16	263,54	86,08	131,8
2019-05-08	May	HO1_1	HO1	0,90 ± 0,12	171,75	155,15	85,88	77,6
2019-05-08	May	HO1_2	HO1	1,59 ± 0,28	93,65	148,78	46,83	74,4
2019-05-30	May	HO1_1	HO1	2,15 ± 0,08	80,67	173,83	40,34	86,9
2019-05-30	May	HO1_2	HO1	2,09 ± 0,18	122,74	256,72	61,37	128,4
2018-09-22	September	HO3_1	HO3	1,45 ± 0,24	124,31	179,64	62,16	89,8
2018-09-22	September	HO3_2	HO3	1,44 ± 0,25	42,84	61,76	21,42	30,9

2018-10-18	October	HO3_1	HO3	1,69 ± 0,22	19,95	33,80	9,98	16,9
2018-10-18	October	HO3_2	HO3	1,97 ± 0,19	6,72	13,25	3,36	6,6
2018-11-05	November	HO3_1	HO3	1,30 ± 0,11	93,32	121,30	46,66	60,6
2018-11-05	November	HO3_2	HO3	1,17 ± 0,25	97,70	113,91	48,85	57,0
2018-11-12	November	HO3_1	HO3	0,24 ± 0,04	8,36	1,99	4,18	1,0
2018-11-12	November	HO3_2	HO3	0,44 ***	20,11	8,78	10,06	4,4
2018-11-20	November	HO3_1	HO3	1,12 ± 0,68	87,21	97,31	43,61	48,7
2018-11-20	November	HO3_2	HO3	0,91 ± 0,19	97,14	88,53	48,57	44,3
2018-11-28	November	HO3_1	HO3	0,92 ± 0,06	59,13	54,43	29,57	27,2
2018-11-28	November	HO3_2	HO3	0,34 ***	27,89	9,47	13,94	4,7
2018-12-11	December	HO3_1	HO3	0,47 ± 0,11	339,32	159,91	169,66	80,0
2018-12-11	December	HO3_2	HO3	0,16 ***	66,67	10,58	33,34	5,3
2018-12-17	December	HO3_1	HO3	1,18 ± 0,12	88,58	104,96	44,29	52,5
2018-12-17	December	HO3_2	HO3	0,97 ± 0,10	111,93	108,53	55,97	54,3
2019-01-03	January	HO3_1	HO3	0,36 ± 0,01	66,16	23,80	33,08	11,9
2019-01-03	January	HO3_2	HO3	0,25 ***	36,69	9,17	18,35	4,6
2019-01-07	January	HO3_1	HO3	0,26 ± 0,07	57,58	15,16	28,79	7,6
2019-01-07	January	HO3_2	HO3	0,25 ***	55,62	13,95	27,81	7,0
2019-01-14	January	HO3_1	HO3	0,89 ± 0,39	66,12	58,54	33,06	29,3
2019-01-14	January	HO3_2	HO3	0,88 ± 0,18	49,11	43,28	24,56	21,6
2019-01-28	January	HO3_1	HO3	1,11 ± 0,49	44,74	49,54	22,37	24,8
2019-02-04	February	HO3_1	HO3	0,88 ± 0,14	487,59	428,93	243,80	214,5
2019-02-04	February	HO3_2	HO3	1,35 ± 0,20	431,29	580,42	215,65	290,2
2019-02-13	February	HO3_1	HO3	0,66 ± 0,06	387,81	256,66	193,91	128,3
2019-02-13	February	HO3_2	HO3	0,34 ± 0,19	40,13	13,58	20,07	6,8
2019-02-21	February	HO3_1	HO3	0,37 ***	65,28	24,24	32,64	12,1
2019-03-14	March	HO3_1	HO3	0,61 ***	18,06	10,96	9,03	5,5
2019-03-28	March	HO3_1	HO3	0,11 ***	75,35	8,12	37,68	4,1
NA	March	NA	NA	0,96 ± 0,10	NA	NA	NA	NA

Date	Month	ID	Analyte	Mean ± SD				
2019-04-01	April	HO3_1	HO3	1,60 ± 0,11	36,99	59,07	18,50	29,5
2019-04-01	April	HO3_2	HO3	0,89 ± 0,14	53,63	47,92	26,82	24,0
2019-04-08	April	HO3_1	HO3	0,52 ± 0,09	69,87	36,32	34,94	18,2
2019-04-08	April	HO3_2	HO3	0,72 ± 0,14	59,92	42,87	29,96	21,4
2019-04-29	April	HO3_1	HO3	0,59 ± 0,25	43,59	25,66	21,80	12,8
2019-04-29	April	HO3_2	HO3	1,30 ± 0,07	31,80	41,23	15,90	20,6
2019-05-07	May	HO3_1	HO3	0,34 ± 0,13	91,91	31,28	45,96	15,6
2018-09-22	September	HO4_1	HO4	0,93 ± 0,07	47,19	43,91	23,60	22,0
2018-09-22	September	HO4_2	HO4	0,58 ± 0,02	66,24	38,67	33,12	19,3
2018-10-12	October	HO4_1	HO4	0,66 ± 0,07	29,13	19,31	14,57	9,7
2018-10-12	October	HO4_2	HO4	1,25 ± 0,17	29,62	37,12	14,81	18,6
2018-11-05	November	HO4_1	HO4	1,49 ± 0,05	37,52	56,02	18,76	28,0
2018-11-05	November	HO4_2	HO4	1,61 ± 0,57	54,48	87,61	27,24	43,8
2018-11-12	November	HO4_1	HO4	0,54 ± 0,00	97,00	52,53	48,50	26,3
2018-11-12	November	HO4_2	HO4	0,87 ± 0,02	24,67	21,36	12,33	10,7
2018-11-28	November	HO4_1	HO4	2,05 ± 0,10	98,97	203,27	49,48	101,6
2018-11-28	November	HO4_2	HO4	0,89 ± 0,15	9,50	8,41	4,75	4,2
2018-12-11	December	HO4_1	HO4	1,27 ± 0,09	97,17	122,99	48,58	61,5
2018-12-11	December	HO4_2	HO4	0,13 ± 0,07	10,44	1,41	5,22	0,7
2018-12-18	December	HO4_1	HO4	0,03 ± ***	22,42	0,68	11,21	0,3
2018-12-27	December	HO4_2	NA	NA ± ***	NA	NA	NA	
2019-01-02	January	HO4_1	HO4	1,29 ± 0,09	58,14	74,73	29,07	37,4
2019-01-02	January	HO4_2	HO4	0,63 ± 0,17	64,15	40,64	32,08	20,3
2019-01-07	January	HO4_1	HO4	2,15 ± 0,03	45,88	98,52	22,94	49,3
2019-01-07	January	HO4_2	HO4	0,56 ± 0,13	19,82	11,10	9,91	5,6
2019-01-28	January	HO4_1	HO4	2,03 ± 0,06	75,12	152,32	37,56	76,2
2019-01-28	January	HO4_2	HO4	0,96 ± 0,21	86,62	83,29	43,31	41,6
2019-02-06	February	HO4_1	HO4	0,16 ± 0,00	89,64	13,98	44,82	7,0
2019-02-06	February	HO4_2	HO4	0,55 ± 0,05	49,72	27,41	24,86	13,7

2019-02-13	February	HO4_1	HO4	0,40	±	0,12	27,49	11,10	13,75	5,6
2019-02-13	February	HO4_2	HO4	0,17	±	0,07	21,40	3,72	10,70	1,9
2019-02-27	February	HO4_1	HO4	1,95	±	0,36	62,60	121,84	31,30	60,9
2019-03-14	March	HO4_1	HO4	3,01	±	0,02	72,83	219,01	36,42	109,5
2019-03-14	March	HO4_2	HO4	0,56	±	0,11	47,16	26,62	23,58	13,3
2019-03-25	March	HO4_2	HO4	0,86	±	0,03	43,41	37,48	21,71	18,7
2019-03-25	March	HO4_1	HO4	0,63	±	0,14	23,71	14,83	11,86	7,4
2019-04-01	April	HO4_1	HO4	0,99	±	0,02	34,91	34,47	17,46	17,2
2019-04-01	April	HO4_2	HO4	0,47	±	0,25	31,48	14,95	15,74	7,5
2019-04-08	April	HO4_1	HO4	0,81	±	0,29	27,29	22,22	13,65	11,1
2019-04-08	April	HO4_2	HO4	0,27	±	0,02	38,32	10,29	19,16	5,1
2019-04-20	April	HO4_1	HO4	0,66		***	65,94	43,38	32,97	21,7
2019-04-20	April	HO4_2	HO4	6,84	±	0,00	46,69	319,18	23,35	159,6
2019-04-29	April	HO4_1	HO4	0,66	±	0,00	26,37	17,38	13,19	8,7
2019-04-29	April	HO4_2	HO4	0,52	±	0,10	22,49	11,62	11,25	5,8
2019-05-07	May	HO4_1	HO4	0,48	±	0,18	20,99	10,17	10,50	5,1
2019-05-07	May	HO4_2	HO4	0,51	±	0,04	16,60	8,50	8,30	4,3
2019-05-29	May	HO4_1	HO4	0,23	±	0,01	20,55	4,63	10,28	2,3
2019-05-29	May	HO4_2	HO4	4,36	±	0,11	28,62	124,87	14,31	62,4

Table B3 Mean Si concentrations and statistical analysis on log transformed data.

Management zone	Water regime		N	Si_M $\mu g\ g^{-1}_{soil}$	Shapiro-Wilk p-value	Levene p-value	N	Si_{Am} $mg\ g^{-1}_{soil}$	Shapiro-Wilk p-value	Levene p-value
Palm circle	Well-drained	HO	4	11,17 ± 5,42	0,68		4	1,71 ± 0,35	0,04	
Oil-palm row	Well-drained	HO	4	6,38 ± 2,85	0,01	0,26	4	1,87 ± 0,51	0,28	0,50
Interrow	Well-drained	HO	3	5,62 ± 0,10	0,80		3	1,88 ± 0,39	0,18	
Frond pile	Well-drained	HO	4	13,68 ± 6,54	1,00		4	3,97 ± 1,54	0,96	
Palm circle	Riparian	HOr	4	10,55 ± 3,06	0,43		4	1,44 ± 0,55	0,87	
Oil-palm row	Riparian	HOr	4	11,94 ± 6,09	0,39	0,89	4	2,08 ± 0,17	0,89	0,15
Interrow	Riparian	HOr	4	11,38 ± 3,74	0,76		4	2,71 ± 0,29	0,14	
Frond pile	Riparian	HOr	4	19,56 ± 6,13	0,65		4	2,96 ± 0,69	0,26	

Mean ± Std. dev., n = 4 and n=3 for HO interrow. Statistics was conducted doing a 1-way ANOVA and Tukey post-hoc test.

Normally distributed data whereby the homogeneity of variances is asserted.

7 Data availability

Data are available upon request to the authors.

8 Supplement

Data is provided in the appendix of the manuscript.

9 Author's contribution

BvL and DS designed the study of the manuscript with input from HH, ST and AT. BG conducted soil sampling with input from BvL, ST, AT, and DS. CS sampled and provided meteorological data. BG conducted laboratory analysis and evaluated the data with input from BvL, HH, CS and DS. BG wrote the first draft. All authors (BG, BvL, HH, CS, ST, AT, and DS) contributed to generating and reviewing the subsequent versions of the paper.

10 Competing interests

The authors declare that they have no conflict of interests.

11 Acknowledgements

We thank the German Research Foundation DFG for funding this project (DFG project no. 391702217). The project was associated to the Collaborative Research Center 990 "Environmental and Socioeconomic Functions of Tropical Lowland Rainforest Transformation Systems" (CRC 990, DFG project no. 192626868). We also thank the Ministry of Education, Technology and Higher Education (RISTEKDIKTI) for granting a research permission in Indonesia and the CRC 990 oil-palm smallholder partners. Soil sampling was conducted using the research permits 110/SIP/FRP/E5/Dit.KI/IV/2018 and 187/ E5/E5.4/SIP/2019. Special thanks go to our Indonesian counterparts, the CRC-990 office members, and our fieldwork assistants Nando, Daniel, Somad and Firdaus in Jambi. We would also like to thank the laboratory staff from the Institute of Geography, University of Göttingen, Jürgen Grotheer, Anja Södje and Petra Voigt, for their support.

12 Financial support

This project was funded by the German Research Foundation DFG (DFG project no. 391702217).

13 References

Albert, R. M., Bamford, M. K. and Esteban, I.: Reconstruction of ancient palm vegetation landscapes using a phytolith approach, Quat. Int., 369, 51–66, doi:10.1016/j.quaint.2014.06.067, 2015.

Alexandre, A., Meunier, J.-D., Colin, F. and Koud, J.-M.: Plant impact on the biogeochemical cycle of silicon and related weathering processes, Geochim. Cosmochim. Acta, 61(3), 677–682, doi:10.1016/S0016-7037(97)00001-X, 1997.

Allen, K., Corre, M. D., Kurniawan, S., Utami, S. R. and Veldkamp, E.: Spatial variability surpasses land-use change effects on soil biochemical properties of converted lowland landscapes in Sumatra, Indonesia, Geoderma, 284, 42–50, doi:10.1016/j.geoderma.2016.08.010, 2016.

Arshad, A. M.: Physical land evaluation for oil palm cultivation in district of Temerloh and Kuantan, Pahang, Peninsular Malaysia., J. Biol. Agric. Heal., 5(4), 104–112, 2015.

Barão, L., Clymans, W., Vandevenne, F., Meire, P., Conley, D. J. and Struyf, E.: Pedogenic and biogenic alkaline-extracted silicon distributions along a temperate land-use gradient, Eur. J. Soil Sci., 65, 693–705, doi:10.1111/ejss.12161, 2014.

Barão, L., Teixeira, R., Vandevenne, F., Ronchi, B., Unzué-Belmonte, D. and Struyf, E.: Silicon Mobilization in Soils: the Broader Impact of Land Use, Silicon, 12, 1529–1538, doi:10.1007/s12633-019-00245-y, 2020.

425 Blecker, S. W., McCulley, R. L., Chadwick, O. A. and Kelly, E. F.: Biologic cycling of silica across a grassland bioclimosequence, Global Biogeochem. Cycles, 20(3), doi:10.1029/2006GB002690, 2006.

Breuning-Madsen, H., Kristensen, J. Å., Awadzi, T. W. and Murray, A. S.: Early cultivation and bioturbation cause high long-term soil erosion rates in tropical forests: OSL based evidence from Ghana, Catena, 151, 130–136, doi:10.1016/j.catena.2016.12.002, 2017.

430 Clough, Y., Krishna, V. V., Corre, M. D., Darras, K., Denmead, L. H., Meijide, A., Moser, S., Musshoff, O., Steinebach, S., Veldkamp, E., Allen, K., Barnes, A. D., Breidenbach, N., Brose, U., Buchori, D., Daniel, R., Finkeldey, R., Harahap, I., Hertel, D., Holtkamp, A. M., Hörandl, E., Irawan, B., Jaya, I. N. S., Jochum, M., Klarner, B., Knohl, A., Kotowska, M. M., Krashevska, V., Kreft, H., Kurniawan, S., Leuschner, C., Maraun, M., Melati, D. N., Opfermann, N., Pérez-Cruzado, C., Prabowo, W. E., Rembold, K., Rizali, A., Rubiana, R., Schneider, D., Tjitrosoedirdjo, S. S., Tjoa, A., Tscharntke, T. and Scheu, S.: Land-use choices follow
435 profitability at the expense of ecological functions in Indonesian smallholder landscapes, Nat. Commun., 7, 1–12, doi:10.1038/ncomms13137, 2016.

Clymans, W., Struyf, E., Van den Putte, A., Langhans, C., Wang, Z. and Govers, G.: Amorphous silica mobilization by inter-rill erosion: Insights from rainfall experiments, Earth Surf. Process. Landforms, 40(9), 1171–1181, doi:10.1002/esp.3707, 2015.

440 Comte, I., Colin, F., Whalen, J. K., Grünberger, O. and Caliman, J.-P.: Agricultural practices in oil palm plantations and their impact on hydrological changes, nutrient fluxes and water quality in Indonesia: a review., 2012.

Conley, D. J., Likens, G. E., Buso, D. C., Saccone, L., Bailey, S. W. and Johnson, C. E.: Deforestation causes increased dissolved silicate losses in the Hubbard Brook Experimental Forest, Glob. Chang. Biol., 14, 2548–
445 2554, doi:10.1111/j.1365-2486.2008.01667.x, 2008.

Corley, R. H. V. and Tinker, P. B.: The Oil Palm, Fifth edit., 2016.

Cornelis, J.-T., Delvaux, B., Georg, R. B., Lucas, Y., Ranger, J. and Opfergelt, S.: Tracing the origin of dissolved silicon transferred from various soil-plant systems towards rivers: a review, Biogeosciences, 8, 89–112, doi:10.5194/bg-8-89-2011, 2011.

450 De Coster, G. L.: The Geology of the central and south sumatra basins, in IPA, 2006 - 3rd Annual Convention Proceedings, 1974, p. 77., 2006.

Darras, K. F. A., Corre, M. D., Formaglio, G., Tjoa, A., Potapov, A., Brambach, F., Sibhatu, K. T., Grass, I., Rubiano, A. A., Buchori, D., Drescher, J., Fardiansah, R., Hölscher, D., Irawan, B., Kneib, T., Krashevska, V., Krause, A., Kreft, H., Li, K., Maraun, M., Polle, A., Ryadin, A. R., Rembold, K., Stiegler, C., Scheu, S., Tarigan,
455 S., Valdés-Uribe, A., Yadi, S., Tscharntke, T. and Veldkamp, E.: Reducing Fertilizer and Avoiding Herbicides in Oil Palm Plantations—Ecological and Economic Valuations, Front. For. Glob. Chang., 2, 1–15, doi:10.3389/ffgc.2019.00065, 2019.

Dislich, C., Keyel, A. C., Salecker, J., Kisel, Y., Meyer, K. M., Auliya, M., Barnes, A. D., Corre, M. D., Darras, K., Faust, H., Hess, B., Klasen, S., Knohl, A., Kreft, H., Meijide, A., Nurdiansyah, F., Otten, F., Pe'er, G.,
460 Steinebach, S., Tarigan, S., Tölle, M. H., Tscharntke, T. and Wiegand, K.: A review of the ecosystem functions in oil palm plantations, using forests as a reference system, Biol. Rev., 92(3), 1539–1569, doi:10.1111/brv.12295, 2017.

Drescher, J., Rembold, K., Allen, K., Beckscha, P., Buchori, D., Clough, Y., Faust, H., Fauzi, A. M., Gunawan, D., Hertel, D., Irawan, B., Jaya, I. N. S., Klarner, B., Kleinn, C., Knohl, A., Kotowska, M. M., Krashevska, V.,
465 Krishna, V., Leuschner, C., Lorenz, W., Meijide, A., Melati, D., Steinebach, S., Tjoa, A., Tscharntke, T., Wick, B., Wiegand, K., Kreft, H. and Scheu, S.: Ecological and socio-economic functions across tropical land use systems after rainforest conversion, Philos. Trans. R. Soc. B Biol. Sci., 371(1694), 20150275, doi:10.1098/rstb.2015.0275, 2016.

Dürr, H. H., Meybeck, M., Hartmann, J., Laruelle, G. G. and Roubeix, V.: Global spatial distribution of natural
470 riverine silica inputs to the coastal zone, Biogeosciences, 8(3), 597–620, doi:10.5194/bg-8-597-2011, 2011.

Epstein, E.: Silicon: its manifold roles in plants, Ann. Appl. Biol., 155(2), 155–160, doi:10.1111/j.1744-7348.2009.00343.x, 2009.

Euler, M., Schwarze, S., Siregar, H. and Qaim, M.: Oil Palm Expansion among Smallholder Farmers in Sumatra, Indonesia, J. Agric. Econ., 67(3), 658–676, doi:10.1111/1477-9552.12163, 2016.

475   Formaglio, G., Veldkamp, E., Duan, X., Tjoa, A. and Corre, M. D.: Herbicide weed control increases nutrient leaching as compared to mechanical weeding in a large-scale oil palm plantation, Biogeosciences, 17(21), 5243–5262, doi:10.5194/bg-2020-153, 2020.

Fraysse, F., Pokrovsky, O. S., Schott, J. and Meunier, J.-D.: Surface chemistry and reactivity of plant phytoliths in aqueous solutions, Chem. Geol., 258, 197–206, doi:10.1016/j.chemgeo.2008.10.003, 2009.

480   Georgiadis, A., Sauer, D., Herrmann, L., Breuer, J., Zarei, M. and Stahr, K.: Development of a method for sequential Si extraction from soils, Geoderma, 209, 251–261, doi:10.1016/j.geoderma.2013.06.023, 2013.

Grass, I., Kubitza, C., Krishna, V. V., Corre, M. D., Mußhoff, O., Pütz, P., Drescher, J., Rembold, K., Ariyanti, E. S., Barnes, A. D., Brinkmann, N., Brose, U., Brümmer, B., Buchori, D., Daniel, R., Darras, K. F. A., Faust, H., Fehrmann, L., Hein, J., Hennings, N., Hidayat, P., Hölscher, D., Jochum, M., Knohl, A., Kotowska, M. M.,
485   Krashevska, V., Kreft, H., Leuschner, C., Lobite, N. J. S., Panjaitan, R., Polle, A., Potapov, A. M., Purnama, E., Qaim, M., Röll, A., Scheu, S., Schneider, D., Tjoa, A., Tscharntke, T., Veldkamp, E. and Wollni, M.: Trade-offs between multifunctionality and profit in tropical smallholder landscapes, Nat. Commun., 11(1), 1–13, doi:10.1038/s41467-020-15013-5, 2020.

Grasshoff, K., Kremling, K. and Ehrhardt, M.: Methods of sea water analysis, third., John Wiley & Sons., 2009.

490   Guillaume, T., Damris, M. and Kuzyakov, Y.: Losses of soil carbon by converting tropical forest to plantations: erosion and decomposition estimated by δ13C, Glob. Chang. Biol., 21(9), 3548–3560, doi:10.1111/gcb.12907, 2015.

Guillaume, T., Holtkamp, A. M., Damris, M., Brümmer, B. and Kuzyakov, Y.: Soil degradation in oil palm and rubber plantations under land resource scarcity, Agric. Ecosyst. Environ., 232, 110–118,
495   doi:10.1016/j.agee.2016.07.002, 2016.

Guntzer, F., Keller, C. and Meunier, J. D.: Benefits of plant silicon for crops: A review, Agron. Sustain. Dev., 32(1), 201–213, doi:10.1007/s13593-011-0039-8, 2012.

Harrison, R. D. and Swinfield, T.: Restoration of logged humid tropical forests: An experimental programme at Harapan Rainforest, Indonesia, Trop. Conserv. Sci., 8(1), 4–16, doi:10.1177/194008291500800103, 2015.

500   Haynes, R. J.: A contemporary overview of silicon availability in agricultural soils, J. Plant Nutr. Soil Sci., 177(6), 831–844, doi:10.1002/jpln.201400202, 2014.

Hennings, N., Becker, J. N., Guillaume, T., Damris, M., Dippold, M. A. and Kuzyakov, Y.: Riparian wetland properties counter the effect of land-use change on soil carbon stocks after rainforest conversion to plantations, Catena, 196, 104941, doi:10.1016/j.catena.2020.104941, 2021.

505   Huisman, S. N., Raczka, M. F. and McMichael, C. N. H.: Palm phytoliths of mid-elevation Andean forests, Front. Ecol. Evol., 6, 1–8, doi:10.3389/fevo.2018.00193, 2018.

Iler, R. K.: The chemistry of silica: solubility, polymerization, colloid and surface properties, and biochemistry, Wiley & Sons., 1979.

Keller, C., Guntzer, F., Barboni, D., Labreuche, J. and Meunier, J.-D.: Impact of agriculture on the Si
510   biogeochemical cycle: Input from phytolith studies, Comptes Rendus Geosci., 344(11–12), 739–746, doi:10.1016/j.crte.2012.10.004, 2012.

Klotzbücher, T., Klotzbücher, A., Kaiser, K., Merbach, I. and Mikutta, R.: Impact of agricultural practices on plant-available silicon, Geoderma, 331, 15–17, doi:10.1016/j.geoderma.2018.06.011, 2018.

Kotowska, M. M., Leuschner, C., Triadiati, T., Meriem, S. and Hertel, D.: Quantifying above- and belowground
515   biomass carbon loss with forest conversion in tropical lowlands of Sumatra (Indonesia), Glob. Chang. Biol., 21(10), 3620–3634, doi:10.1111/gcb.12979, 2015.

Kraushaar, S., Konzett, M. and Meister, J.: Suitability of phytoliths as a quantitative process tracer for soil erosion studies., 2021.

Laumonier, Y.: The Vegetation and Physiography of Sumatra, in Geobotany, vol. 22, p. 223, Kluwer Academic Publishers., 1997.

von der Lühe, B., Pauli, L., Greenshields, B., Hughes, H. J., Tjoa, A. and Sauer, D.: Transformation of Lowland Rainforest into Oil-palm Plantations and use of Fire alter Topsoil and Litter Silicon Pools and Fluxes, Silicon, 13(12), 4345–4353, doi:10.1007/s12633-020-00680-2, 2020.

Luke, S. H., Purnomo, D., Advento, A. D., Aryawan, A. A. K., Naim, M., Pikstein, R. N., Ps, S., Rambe, T. D. S., Soeprapto, Caliman, J.-P., Snaddon, J. L., Foster, W. A. and Turner, E. C.: Effects of understory vegetation management on plant communities in oil palm plantations in Sumatra, Indonesia, Front. For. Glob. Chang., 2, 1–13, doi:10.3389/ffgc.2019.00033, 2019.

Ma, J. F. and Takahashi, E.: Silicon-accumulating plants in the plant kingdom, in Soil, fertilizer, and plant silicon research in Japan, pp. 63–71, Elsevier Science, Amsterdam., 2002.

Meijaard, E., Brooks, T., Carlson, K. M., Slade, E. M. and Ulloa, J. G.: The environmental impacts of palm oil in context, Nat. plants, 6(12), 1418–1426, doi:10.1038/s41477-020-00813-w, 2020.

Meunier, J. D., Keller, C., Guntzer, F., Riotte, J., Braun, J. J. and Anupama, K.: Assessment of the 1% Na2CO3 technique to quantify the phytolith pool, Geoderma, 216, 30–35, doi:10.1016/j.geoderma.2013.10.014, 2014.

Munevar, F. and Romero, A.: Soil and plant silicon status in oil palm crops in Colombia, Exp. Agric., 51(3), 382, doi:10.1017/S0014479714000374, 2015.

Oliveira, P. T. S., Wendland, E. and Nearing, M. A.: Rainfall erosivity in Brazil: a review, Catena, 100, 139–147, doi:10.1016/j.catena.2012.08.006, 2013.

Qaim, M., Sibhatu, K. T., Siregar, H. and Grass, I.: Environmental, Economic, and Social Consequences of the Oil Palm Boom, Annu. Rev. Resour. Econ., 12(1), 1–24, doi:10.1146/annurev-resource-110119-024922, 2020.

Quigley, K. M., Donati, G. L. and Anderson, T. M.: Variation in the soil 'silicon landscape' explains plant silica accumulation across environmental gradients in Serengeti, Plant Soil, 410(1–2), 217–229, doi:10.1007/s11104-016-3000-4, 2017.

Sauer, D., Saccone, L., Conley, D. J., Herrmann, L. and Sommer, M.: Review of methodologies for extracting plant-available and amorphous Si from soils and aquatic sediments, Biogeochemistry, 80(1), 89–108, doi:10.1007/s10533-005-5879-3, 2006.

Schaller, J. and Puppe, D.: Heat improves silicon availability in mineral soils, Geoderma, 386(August 2020), 114909, doi:10.1016/j.geoderma.2020.114909, 2021.

Schaller, J., Frei, S., Rohn, L. and Gilfedder, B. S.: Amorphous silica controls water storage capacity and phosphorus mobility in soils, Front. Environ. Sci., 8, 94, doi:10.3389/fenvs.2020.00094, 2020.

Schaller, J., Puppe, D., Kaczorek, D., Ellerbrock, R. and Sommer, M.: Silicon cycling in soils revisited, Plants, 10(2), 1–36, doi:10.3390/plants10020295, 2021.

Sinukaban, N., Tarigan, S. D., Purwakusuma, W., Baskoro, D. P. T. and Wahyuni, E. D.: Analysis of watershed function sediment transfer across various type of filter strips., 2000.

Street-Perrott, F. . A. and Barker, P. A.: Biogenic silica: a neglected component of the coupled global continental biogeochemical cycles of carbon and silicon, Earth Surf. Process. Landforms, 33(9), 1436–1457, doi:10.1002/esp.1712 F., 2008.

Struyf, E. and Conley, D.: Emerging understanding of the ecosystem silica filter, Biogeochemistry, 107, 9–18, doi:10.1007/s10533-011-9590-2 SYNTHESIS, 2012.

Struyf, E. and Conley, D. J.: Silica: an essential nutrient in wetland biogeochemistry, Front. Ecol. Environ., 7(2), 88–94, doi:10.1890/070126, 2009.

Struyf, E., Smis, A., Van Damme, S., Garnier, J., Govers, G., Van Wesemael, B., Conley, D. J., Batelaan, O.,

Frot, E., Clymans, W., Vandevenne, F., Lancelot, C., Goos, P. and Meire, P.: Historical land use change has lowered terrestrial silica mobilization, Nat. Commun., 1(1), 1–7, doi:10.1038/ncomms1128, 2010.

Tarigan, S., Stiegler, C., Wiegand, K., Knohl, A. and Murtilaksono, K.: Relative contribution of
565   evapotranspiration and soil compaction to the fluctuation of catchment discharge: case study from a plantation landscape, Hydrol. Sci. J., 65(7), 1239–1248, doi:10.1080/02626667.2020.1739287, 2020.

de Tombeur, F., Turner, B. L., Laliberté, E., Lambers, H., Mahy, G., Faucon, M. P., Zemunik, G. and Cornelis, J. T.: Plants sustain the terrestrial silicon cycle during ecosystem retrogression, Science (80-.)., 369, 1245–1248, doi:10.1126/science.abc0393, 2020.

570   Tsujino, R., Yumoto, T., Kitamura, S., Djamaluddin, I. and Darnaedi, D.: History of forest loss and degradation in Indonesia, Land use policy, 57, 335–347, doi:10.1016/j.landusepol.2016.05.034, 2016.

Unzué-Belmonte, D., Ameijeiras-Mariño, Y., Opfergelt, S., Cornelis, J.-T., Barão, L., Minella, J., Meire, P. and Struyf, E.: Land use change affects biogenic silica pool distribution in a subtropical soil toposequence, Solid Earth, 8, 737–750, doi:10.5194/se-8-737-2017, 2017.

575   Vandevenne, F., Struyf, E., Clymans, W. and Meire, P.: Agricultural silica harvest: have humans created a new loop in the global silica cycle ?, Front. Ecol. Environ., 10(5), 243–248, doi:10.1890/110046, 2012.